Smart coordination of virtual energy storage systems for distribution network management

Dongxiao Wang[a], Chun Sing Lai[a,b,*], Xuecong Li[a], Runji Wu[a], Xiaodan Gao[c], Loi Lei Lai[a],

Xueqing Wu[d], Yi Xu[d], Yonggang Wen[e], Alfredo Vaccaro[f]

[a] Department of Electrical Engineering, School of Automation, Guangdong University of Technology, Guangzhou, China

[b] School of Civil Engineering, Faculty of Engineering and Physical Sciences, University of Leeds, Leeds, LS2 9JT, United Kingdom

[c] Lloyd's Register, Melbourne, Australia

[d] Guangdong Foshan Power Construction Corporation Group Co., Ltd., Foshan, China

[e] School of Computer Engineering, Nanyang Technological University, Singapore

[f] Department of Engineering (DING), University of Sannio, Benevento, Italy

*Corresponding author email: c.s.lai@leeds.ac.uk

ABSTRACT: With increasing penetration of solar photovoltaic (PV) resources in distribution networks, voltage regulation becomes an important issue. In addition, due to the growth in air conditioning load in summer days, overloading management draws researchers' attentions as well. This paper proposes a two-level consensus-driven distributed control strategy to coordinate virtual energy storage systems (VESSs), i.e. residential households with air conditioners, to avoid the violation of voltage and loading which are regarded as part of the main power quality issues in future distribution network. In the lower level, the precise modelling of VESSs is firstly built, then VESSs are aggregated via aggregators for better participating in the control scheme. Once the violation occurs, a consensus-driven control scheme in the upper level will be initiated to eliminate the error. Required active power adjustment is shared among VESSs aggregators via sparse communication networks, without compromising end users' thermal comfort. Changes in the dynamic communication network topology are investigated in this paper to demonstrate their impacts on system performance. Simulation results based on a practical system in New South Wales, Australia is used to demonstrate the proposed control scheme, which can effectively manage voltage and loading in a distribution network with scalability and robustness.

Keywords— Consensus Algorithm, Network Loading Management, Network Voltage Regulation, Smart Distribution Network, Virtual Energy Storage Systems

1. Introduction

As an effective solution to future energy crisis, renewable energy resources are playing a vital role in current power systems. Based on the electricity forecast of International Energy Agency (IEA), the share of renewable energy in meeting global power demand would reach to almost 30% in 2023, up from 24% in 2017 [1]. During this period, more than 70% of global electricity generation growth is met by renewables, led by solar PV. Solar PV brings unprecedented environmental and technical benefits, such as low carbon emissions and congestion management. Nevertheless, the large-scale penetration of PV energy in distribution network causes many power quality issues as well, such as harmonic pollution [2] and voltage rise [3]. According to [3], voltage rise is the most significant one among the power quality issues in distribution network. Overvoltage problem usually occurs

at the time of high PV penetration periods and light load periods [4]. In contrast, undervoltage happens at the time of low PV penetration periods and heavy load periods.

1.1. Related Work

Previous researchers have proposed a variety of techniques on regulating voltage in distribution networks, such as installing voltage regulators [5], changing line impedances and conductor size [6], modulating the tap set points of secondary transformer [7], applying reactive power compensation in PV inverters [8], and reducing solar power generation amount [9], [10] and employing battery energy storage systems (BESSs) [4, 11]. Owing to the randomness of PV energy and customer load, the former three methods require frequent changes of set point and are not flexible for the utility side. By contrast, the latter three methods are based on end-user side and more promising to regulate voltage. However, unavoidable shortcomings still exist here. For example: 1) the distribution network usually has high R/X ratio, therefore, reactive power compensation is not effective enough [3]; 2) in terms of PV generation reduction, the energy efficiency is reduced via this method; 3) although the BESS cost has dropped, customers still bear financial burden on installing large energy storage systems [12]-[14].

Except for voltage regulation, loading management is another important issue in distribution network due to the increasing energy-hungry appliances [15]. Especially in recent years, air conditioners are rapidly making the way to households because of summer heat and falling upfront cost. In line with an investigation led by Ausgrid [16], air conditioners contribute more than half of the load in some of their substations in summer days. If such demand comes up to certain ratio of feeder load, challenges would be imposed to system operation. Network infrastructure capacity needs to be upgraded by system operator to maintain reliable electricity supply. Consequently, billions of dollars would be spent for network upgrading to deal with the short but sharp peak load period. Nevertheless, the infrastructure upgrading is only used for short periods of the year to meet peak demand, which is not cost-effective for system operators.

How to address the noted issues (i.e. voltage regulation and loading management) in a technically and economically efficient manner needs to be considered by the researchers. With the popularity of demand response (DR) technologies, an alternative way to address peak load is through DR programs by shaping the load curve for optimal use of energy and improving asset investment overall efficiency [17]-[20]. In fact, the pressure on integrating large-scale PV resources into distribution network can be alleviated as well with the help of DR programs. Owing to rapid progress in control and communication techniques, thermostatically controlled loads (TCLs) in end-user side can be equipped with control modules to be better involved in DR programs. Among various types of TCLs, air conditioners receive researchers' increasing attentions because they have relatively fast response time with least end-user disruptions and mainly contribute the summer peak load. When air conditioners are turned on/off, the room temperature can maintain within certain range by storing large amount of heat/cold air. This phenomenon is referred as thermal inertia, which is defined as a thermal mass being capable to resist the change on its temperature faced with the fluctuation of ambient temperature [21]. Consequently, a household can shift its energy consumption over the planning horizon to help consume the peak PV generation amount or reduce the peak load periods. The thermal buffering capacity in an air-conditioned household can imitate the energy buffering characteristics of physical energy storage systems, such as batteries, and hence can be viewed as virtual energy storage systems (VESSs). In fact, the air-conditioned household becomes a battery.

The concept of VESSs is not new. Researchers in [22, 23] have taken the flexible loads in power systems as VESSs. In [22], Meng et al. coordinated DR from domestic refrigerator to form the VESS, aiming to provide frequency service for the system. In [23], the author employed virtual energy storage through distributed control

of flexible loads, which was believed to be innovative solutions for integrating renewables. VESSs can be integrated with other energy resources to provide desired services for the system operator. Therefore, distribution utilities are encountering new opportunities in the situation of growing number of air conditioners and increasing penetration of PV resources at customer side. By coordinating VESSs, network voltage regulation and overloading issues can be solved in an efficient and economical way.

This work is inspired by the fact that air conditioners at end-user side are contributing summer peak loads in distribution network and the voltage regulation is necessary with growing PV penetration in customer side. If large number of air-conditioned households is coordinated by DR programs, they can be viewed as VESSs and offer significant system support. Hence, the objective of this work is to put forward an innovative method to regulate distribution network with the help of VESSs. Previous research mainly focused on the adoption of battery storage for supporting stable operation of power systems, which is inferior in terms of economics and flexibility [24, 25]. By utilizing virtual storage systems instead of practical battery storage systems, distribution system operator would reduce the infrastructure investment to a large extent, as well as gain much more flexibility given the fast growth of customer demand and renewable resources penetration.

1.2. Main Contributions

In this paper, a two-level dispatch strategy is proposed to share the required active power adjustment among VESSs for voltage regulation and overloading management. Specifically, in the lower level, the more precise VESS model is built to reflect the dynamic thermal process of air-conditioned households. Given a single VESS has limited capacity to participate in DR program, a group of VESSs in a residential district are aggregated to an aggregator for effective involvement in the control scheme. In the upper level, a consensus-driven distributed control strategy is adopted to fairly regulate system voltage and loading. Compared with centralized control scheme, distributed control shares information through a limited communication network, thus it is more robust against communication failure and is more efficient in coordinating the available units in the system. Among the various types of distributed control schemes, consensus control is a typical approach to achieve the common objective by operating in the same manner via information exchange [26]. Consensus control has been widely applied in microgrids and distribution systems, such as loading shedding [27], frequency regulation [28], and power sharing [29]. In this paper, if the voltage and network loading violate certain limits, the consensus-driven distributed control will coordinate the active power to support system voltage and loading. Compared with existing works in the literature, the contributions of this paper are detailed in two aspects:

(1) The first contribution is the application of VESS, i.e. air-conditioned households, on voltage regulation and overloading management in distribution network. In contrast to conventional energy storage systems, VESSs effectively support system operation with far less cost.

(2) The other contribution is applying a distributed consensus control on distribution network management with high robustness and scalability. The influences of dynamic communication network topology changes on system performance are investigated. Through exchanging information with neighbouring aggregators via sparse communication networks, the active power support is fairly shared among participating aggregators.

The remaining parts of the paper are as follows. VESS modelling, aggregation and coordination strategy are introduced in Section 2. Section 3 presents the proposed control approach, including overloading management and voltage regulation strategies. In Section 4, case studies are carried out and simulation results are analysed to demonstrate the performance of the proposed method scheme. Conclusions and future works are given in Section 5.

2. VESS modelling, aggregation, and coordination strategy

In this section, the thermal modelling of VESS is firstly introduced, followed by the aggregation method. In the last subsection, the VESS coordination strategies are given.

2.1. VESS modelling

In order to capture the thermal behaviour of VESS, the fundamental part is to build a comprehensive thermal model for air-conditioned household. Previous researchers have developed different complexities of thermal models to represent the thermal process of TCLs. In [30] and [31], the authors proposed the first order differential equation to build the individual TCL model. However, this method cannot reflect the actual thermal process of heating, ventilating, and air-conditioning (HVAC) systems owing to the inherent large thermal mass temperature dynamics. In this simplified model, as shown in Fig. 1(a), only ambient temperature, indoor air temperature and thermal resistance are considering, but neglecting explicit model of building materials (especially walls). In fact, indoor air temperature is not only subject to the difference between indoor and outdoor air, but also depends on the thermal energy exchange with internal walls and participations. The thermal mass inside the building has significant temperature variation influenced by external environment, hence could greatly impact the indoor air temperature.

In this paper, a two-parameter thermal model is built to more precisely capture the thermal dynamics of an air-conditioned building, as shown in Fig. 1(b). In this model, the building is divided into two inter-connected parts. One is in-house part, and the other one is the additional thermal mass part with significant thermal capacity, such as walls. The efficiency of a two-parameter thermal model has been proved by [32], where the authors compared the impacts of different complexities of thermal model on indoor air calculation. Thermal dynamic process of VESS can be depicted by:
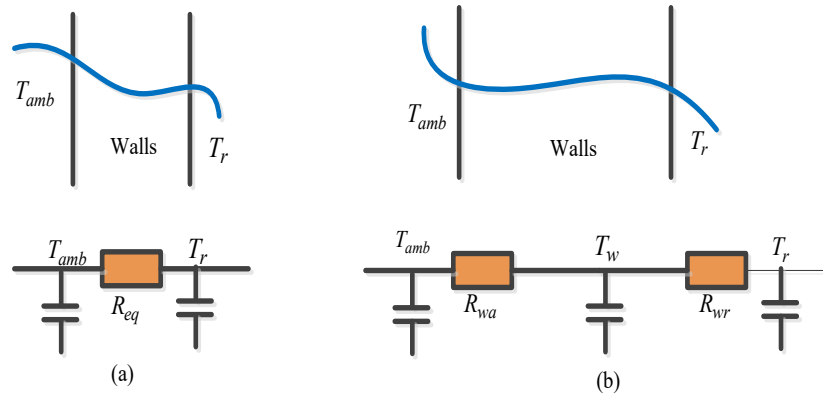
Fig. 1. Schematic of VESS models: (a). one-parameter model (b). two-parameter model.

$$\frac{dT_r(t)}{dt} = \frac{1}{M_a \times Cp_a}\left[\frac{dQ_{gain\_a}(t)}{dt} - \frac{dQ_{ex\_w\_r}(t)}{dt} - \frac{dQ_{ac}(t)}{dt}\right] \tag{1}$$

$$\frac{dT_w(t)}{dt} = \frac{1}{M_w \times Cp_w}\left[\frac{dQ_{gain\_w}(t)}{dt} + \frac{dQ_{ex\_w\_r}(t)}{dt}\right] \tag{2}$$

$$\frac{dQ_{gain\_a}(t)}{dt} = \frac{T_{amb} - T_r}{R_{eq}} \tag{3}$$

$$\frac{dQ_{ex\_w\_r}(t)}{dt} = \frac{T_w - T_r}{R_{wr}} \tag{4}$$

$$\frac{dQ_{gain\_w}(t)}{dt} = \frac{T_{amb} - T_w}{R_{wa}} \tag{5}$$

$$\frac{dQ_{ac}(t)}{dt} = \frac{P_{ac}}{\eta} \tag{6}$$

where, t refers to time; T_r, T_w, and T_{amb} are indoor air temperature, wall temperature, and ambient temperature, respectively; M_a and M_w are mass of indoor air and wall; Cp_a and Cp_w are the thermal capacity of indoor air and wall; Q_{gain_a} and Q_{gain_w} are the heat absorbed by indoor air from the ambient and heat absorbed by the wall from the ambient; $Q_{ex\_w\_r}$ is the heat exchange between indoor air and the wall; Q_{ac} is the cooling energy from air conditioners; R_{eq}, R_{wa}, and R_{wr} are the equivalent thermal resistance of house envelope, the equivalent thermal resistance between ambient and wall outer surface, and the equivalent thermal resistance between indoor air and wall inner surface, respectively; η is the air conditioner performance coefficient; P_{ac} is the air conditioner rated power.

Equations (1)-(2) represent indoor air temperature and wall temperature change rate. Equations (3)-(6) represent heat absorption rate between ambient and indoor air, heat exchange rate between wall and indoor air, heat absorption rate between wall and indoor air, and air conditioner cooling rate respectively. To conveniently calculate indoor air temperature and build a flexible operational planning scheme, the proposed dynamic thermal model can be linearized as below [21]:

$$T_r(t) = \left(1 - \frac{1}{M_a Cp_a R_{eq}}\right) T_r(t-1) + \frac{1}{M_a Cp_a R_{eq}} T_{amb}(t-1) + \frac{T_w(t-1) - T_r(t-1)}{M_a Cp_a R_{wr}} - S_{ac}(t) \frac{Q_{ac}(t-1)}{M_a Cp_a}, \forall t \in [1, N] \tag{7}$$

$$T_w(t) = T_w(t-1) + \frac{T_{amb}(t-1) - T_w(t-1)}{M_w Cp_w R_{wa}} + \frac{T_r(t-1) - T_w(t-1)}{M_w Cp_w R_{wr}}, \forall t \in [1, N] \tag{8}$$

where, N is the total time steps; S_{ac} is air conditioner operation status. 1 means air conditioner is ON, 0 means air conditioner is OFF. The operation status of air conditioners is determined by a thermostatic switching law with the predetermined temperature deadband:

$$S_{ac}(t) = \begin{cases} 0 & \text{if } S_{ac}(t-1) = 1 \,\&\, T_r < T_r^{\min} \\ 1 & \text{if } S_{ac}(t-1) = 0 \,\&\, T_r > T_r^{\max} \\ S_{ac}(t-1) & \text{otherwise} \end{cases} \tag{9}$$

$$T_r^{\min} = T_{set} - \frac{T_{db}}{2}; \quad T_r^{\max} = T_{set} + \frac{T_{db}}{2} \tag{10}$$

where, $T_r^{\min}$, $T_r^{\max}$ refer to the lower and upper limits of indoor air temperature; T_{set} is customer preferred temperature set point; T_{db} represents the temperature deadband scope. To guarantee the thermal comfort of end-users, the indoor air temperature should be restricted as:

$$T_r^{\min} \le T_r(t) \le T_r^{\max} \tag{11}$$

In addition, wall temperature should meet the lower and upper limits:

$$T_w^{\min} \le T_w(t) \le T_w^{\max} \tag{12}$$

2.2. VESS aggregation

Due to the limited thermostatically controlled load amount an individual VESS can provide, its contribution volume usually cannot meet the minimum load requirement for participating demand response programs. Therefore, it is a good practice to aggregate the individual VESS through an aggregator, so that the benefits of DR programs can be effectively reaped. In this work, each residential community comprised of hundreds of air-conditioned households is regulated by an aggregator. The aggregated energy consumption of VESSs is denoted as:

$$P_{VESSs}(t) = \sum_{j=1}^{N_{air}} \frac{1}{\eta_j} P_{ac,j} S_{ac,j}(t)$$

(13)

where, P_{VESSs} means the overall power consumption of aggregated VESSs; N_{air} is the total air conditioner number in the aggregator; j means the jth air conditioner.

To characterize a group of VESSs and further aggregate them, heterogeneous operating scenarios (i.e. different T_{set}, T_{db}, $P_{rate,j}$, etc.) are generated by Monte-Carlo simulation [33]. By generating multiple building model cases within the intermittency range, the practical air-conditioned household scenarios are modelled. For example, the parameters of an air-conditioned household model can be: house length is 13 m, house width is 12 m, house height is 5 m, wall width is 0.25 m, set point of thermostat is 24.5 °C, number of windows is 4, and air conditioner rated power is 4 kW.

After building the aggregation model, the maximum controllable capacity of each VESSs aggregator should be estimated for the upper level control.

Objective:

$$\text{Maximize} \quad P_i^{\max}(t) = \sum_{j=1}^{N_{air}} \frac{1}{\eta_j} \left(1 - S_{ac,j}(t)\right) P_{rate,j}$$

(14)

where, $P_i^{\max}$ refers to the maximum controllable capacity in aggregator i. It is assumed that reactive power is fully compensated in air conditioner side, hence $P_i^{\max}$ specifically means the maximum controllable active power in the aggregator. It is worth noting that the decision variable in (14) is $S_{ac,j}(t)$, and hundreds of VESSs are controlled by the same aggregator.

The calculation of (14) should meet the following conditions:

Subject to:

$$S_{ac}(t) = \begin{cases} 0 & \text{if } S_{ac}(t-1) = 1 \ \& \ T_r < T_r^{\min} \\ 1 & \text{if } S_{ac}(t-1) = 0 \ \& \ T_r > T_r^{\max} \\ S_{ac}(t-1) & \text{otherwise} \end{cases}$$

(15a)

$$T_r^{\min} \le T_r(t) \le T_r^{\max}$$

(15b)

$$T_w^{\min} \le T_w(t) \le T_w^{\max}$$

(15c)

The maximum capacity estimation model in (14) is a nonlinear mix-integer programming problem, which is difficult to be solved by conventional mathematical methods. Therefore, heuristic-based programming methods are employed in this paper to solve the capacity estimation model. After getting the maximum controllable active power in the aggregator, it can be further utilized in the upper level control for voltage regulation and loading management.

2.3. VESS coordination strategies

In this part, the VESS coordination strategies are presented to demonstrate the VESS monitoring, communication and dispatching procedures. The detailed procedures are given below:

(1) Initialization. End users' thermal comfort can be obtained via from collecting historical data based on different weather scenarios or via the collection of household surveys regarding end users' preferences on indoor temperature, relative humidity, etc.

(2) Monitoring. Home energy management system (HEMS) in the air-conditioned household can monitor the room temperature and air conditioner status in real-time, and interact with the smart meter wirelessly.

(3) Estimation. After receiving the relevant information, smart meters then send it to the aggregator for estimating the maximum controllable active power at the current status through the heuristic approach. The estimated maximum controllable power information can be further transferred to the upper level for participating in the distribution network management.

(4) Communication and Dispatch. In the upper level control scheme, the required active power support information will be shared among interconnected aggregators through the communication network in an iterative manner (the detailed control strategy will be illustrated in next section). Once an equilibrium point is achieved, the aggregator would meet its power adjustment commitment to the utility by informing its HEMSs to selectively turn ON/OFF air conditioners.

The proposed hierarchical coordination strategy of aggregated VESSs for distribution network is illustrated in Fig. 2. In order to encourage the participation of end customers on DR programs, participants will receive financial reimbursement from the utility, such as cash reward and reduced electricity price. Note that the frequent motor starting has been recognized as a major cause of flicker, especially for large-scale motors connected to distribution network. To keep the system dynamic stability, especially mitigate voltage fluctuations, reducing the starting current of a motor is one effective measure. A series of starting techniques can be employed, such as using power electronic soft starter and full inverter control of motors.
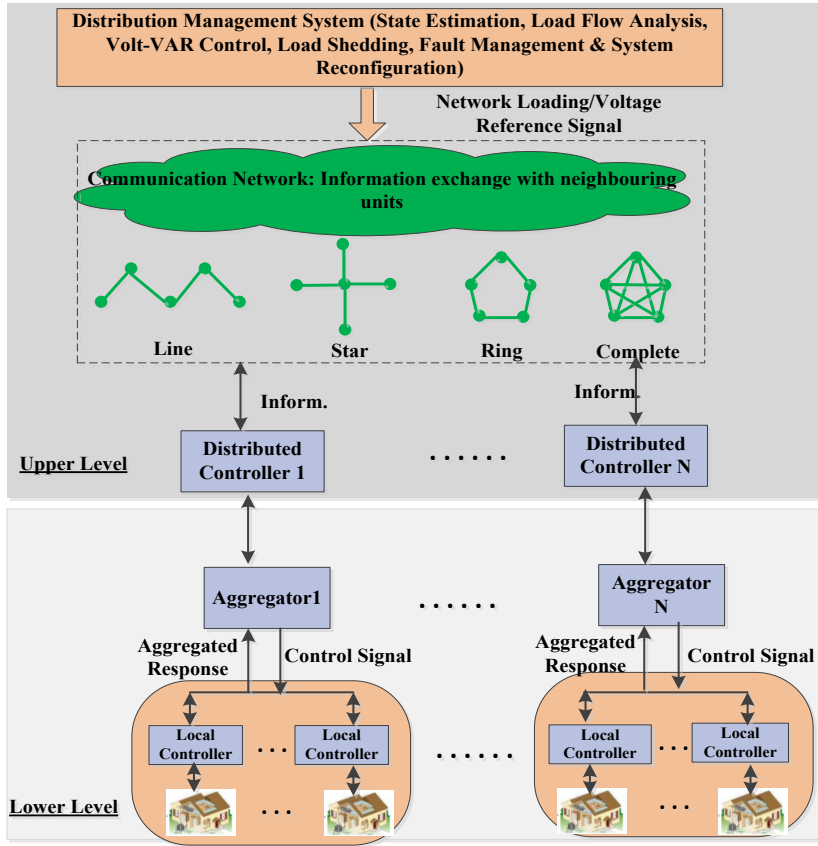
Fig. 2. Proposed hierarchical coordination strategy of aggregated VESSs for distribution network.

3. Proposed approach for network loading and voltage management by VESSs

In this section, through the coordination of aggregated VESSS, a new method to regulate distribution network loading and voltage is proposed. By reducing the active power consumption in peak demand time, the overloading is curtailed, as well as preventing the occurrence of undervoltage. For overvoltage regulation, VESS helps increasing the active power consumption in peak PV generation periods, thus over generated solar power can be consumed to eliminate voltage rise.

To guarantee the active participation in the control scheme, except for the financial incentives for VESSs, the active power curtailment and consumption should be implemented fairly among participating VESSS. Therefore, a consensus decision making method is needed to reach an agreement among all aggregators without a bidding strategy [34, 35]. The detailed control schemes will be introduced in the following subsections.

3.1. Network loading management strategy

For a multi-agent system, the information exchange among agents can be denoted by a weighted graph $G=(V, E, A)$. Introduction for graph theory is omitted here, which can be found in many previous research [15].

Considering the disturbance in communication channels, link failures are likely to happen, thus the static communication network is not appropriate to reflect its dynamics. Here a time varying coefficient matrix is given to model the complete network topology between aggregators and disclose the dynamic change characteristic. The communication matrix is defined as:

$$\Psi(t) = \begin{bmatrix} \psi_{11}(t) & \psi_{12}(t) & \cdots & \psi_{1m}(t) \\ \psi_{21}(t) & \psi_{22}(t) & \cdots & \psi_{2m}(t) \\ \vdots & \vdots & \vdots & \vdots \\ \psi_{m1}(t) & \psi_{m2}(t) & \cdots & \psi_{mm}(t) \end{bmatrix} \tag{16}$$

where, $\psi_{ij}(t)$ reflects the communication link between ith and jth aggregator at time t. $\psi_{ij}=1$ if there is directed communication link between aggregator i and aggregator j, otherwise $\psi_{ij}=0$. Moreover, $\psi_{ii}=1$ for all aggregators. Hence, for a given connected network, the dynamic network topology can be reflected in the adjacency matrix by its values change with time. According to [35], the consensus state will converge to the same value if a spanning tree exists in the communication graph, and the Laplace matrix of the communication graph has a simple zero eigenvalue, and all the other eigenvalues with positive real parts.

In the proposed control scheme, a virtual leader is assigned to define the primal information state via the measurement of critical point [34]. The power exchange between the substation and the main grid is continually monitored by the virtual leader, which is further used as the input control signal of distributed controller for network loading management. The distributed controller will be initiated once the apparent power constraint $S(t) \leq S^{max}$ is violated. The information state of the virtual leader is defined as:

$$\eta_0(t) = K_p m(t) + K_i \sum_{k=0}^{t} m(t) + K_d \left[m(t) - m(t-1) \right] \tag{17}$$

where, $m(t) = S^{max} - S(t)$; $\eta_0(t)$ is the virtual leader initial information state; K_p, K_i, and K_d are the proportional, integral and derivative gains respectively, whose values are given as $K_p=0.66$, $K_i=0.001$, and $K_d=31$, respectively by trial and error methods [4]. The adoption of virtual leader can greatly relieve the heavy computational burden in the control centre given that only virtual leader needs to communicate with the distribution network management system. The information state from the virtual leader will be sent to the connected aggregators at discrete time step.

By using the communication matrix in (16), a transition weight between aggregator i and aggregator j can be defined as:

$$\Gamma_{ij}(t) = \frac{\psi_{ij}(t)}{\sum_{j \in I_i} \psi_{ij}(t)} \tag{18}$$

Γ_{ij} mathematically represents the communication relevance between i and j, and directly determines the convergence speed.

In terms of followers, the consensus-based control scheme will be achieved iteratively. The information state of follower aggregators will be decided based on the states of virtual leader and neighboring aggregators. According to consensus algorithm [37], the consensus state of follower aggregators is updated as:

$$\eta_i(t) = \eta_i(t-1) + \sum_{j \in I_i} \Gamma_{ij}(t-1) \left[\eta_j(t-1) - \eta_i(t-1) \right] \tag{19}$$

where, I_i is the neighbors of aggregator i. With (19), each aggregator could update its consensus state to adjust the active power commitment and finally converge to a unique equilibrium point, denoted as:

$$\frac{P_1}{P_1^{max}} = \frac{P_2}{P_2^{max}} = \cdots = \frac{P_i}{P_i^{max}} = \cdots = \frac{P_n}{P_n^{max}} = \eta_i \tag{20}$$

where, P_i is the required active power commitment for aggregator i; P_i^{max} is the maximum controllable active power in aggregator i, which is derived by the aggregation model in (14).

Therefore, the required active power commitment for network loading management for aggregator i is calculated as:

$$P_i(t) = \eta_i(t) P_i^{max}(t) \tag{21}$$

3.2. Voltage regulation strategy

During normal hours, the bus voltage is kept within normal voltage range considering the constant balance between electricity load and electricity generation. However, bus voltages are easily drifting out of the standard voltage deviation ranges (i.e. normally 5%-10% deviation based on different national standards) at high PV generation and light load periods. Therefore, the objective for voltage regulation is to control the local bus voltage within the acceptable range:

$$V^{min} \leq V_i(t) \leq V^{max} \tag{22}$$

where, $V_i(t)$ is bus i voltage at time t; V^{min} and V^{max} are the minimum and maximum acceptable voltage limits respectively.

Once the voltage limitation occurs, the distributed control scheme will be initiated:

$$\begin{cases} \varepsilon_i(t) = g_i \left[V_i(t) - V_i^{max} \right] \\ \varepsilon_i(t) = g_i \left[V_i(t) - V_i^{min} \right] \end{cases} \tag{23}$$

where, ε_i is the information state for aggregator i; g_i is the weight for bus i. Note that the voltage limit violation is a localized problem, not a network wide one. Therefore, the distributed control strategy is well suited [38].

The relationship between bus voltage change and power change can be represented by Jacobian matrix:

$$\begin{bmatrix} \Delta P \\ \Delta Q \end{bmatrix} = \begin{bmatrix} J_1 & J_2 \\ J_3 & J_4 \end{bmatrix} \cdot \begin{bmatrix} \Delta \theta \\ \Delta |V| \end{bmatrix} \tag{24}$$

where

$$\begin{bmatrix} \Delta \theta \\ \Delta |V| \end{bmatrix} = \begin{bmatrix} J_1 & J_2 \\ J_3 & J_4 \end{bmatrix}^{-1} \begin{bmatrix} \Delta P \\ \Delta Q \end{bmatrix} = \begin{bmatrix} A & B \\ C & D \end{bmatrix} \begin{bmatrix} \Delta P \\ \Delta Q \end{bmatrix} \tag{25}$$

Given that reactive power is fully compensated in this paper and active power considerably affects the voltage magnitude in distribution networks, the approximate sensitivity of bus voltage to power can be given by:

$$\frac{\partial V}{\partial P} = C \tag{26}$$

With the proposed communication structure, the aggregator is only aware of C_{ji} corresponding to their neighbors. Hence, the sensitivity matrix is defined as:

$$\overline{C_{ji}} = \begin{cases} C_{ji} & i \in \{I_j \cup j\} \\ 0 & i \notin \{I_j \cup j\} \end{cases} \tag{27}$$

where, I_j is the neighbors of aggregator j, with which j can communicate with. The transition weight in voltage regulation is given by:

$$\Gamma_{ij}(t) = \frac{\overline{C_{ji}} \psi_{ij}(t)}{\sum\limits_{j=1}^{n} \overline{C_{ji}} \psi_{ji}(t)} \tag{28}$$

The control actions for the aggregator are determined subject to local voltage and its neighbors' information state. The information state of each aggregator is updated at discrete time step as:

$$\varepsilon_i(t) = \Gamma_{ii}(t)\varepsilon_i(t) + \sum_{j \in I_i} \Gamma_{ij}(t)\varepsilon_j(t-1) \tag{29}$$

Finally, the required active power commitment for voltage regulation for aggregator i is defined as:

$$P_i(t) = \varepsilon_i(t)P_i^{max}(t) \tag{30}$$

Comparing the active power commitment in (30) with the active power in (21), the larger value should be chosen in the control scheme in case that undervoltage violation and network overloading occur simultaneously. By choosing a larger value, both violations can be refrained and system normal operation can be guaranteed. To better understand the operation conditions for network loading management and voltage regulation, Fig. 3 has been given here.

The control flowchart for network loading management and voltage regulation is further shown in Fig. 4. The solid blue line means the aggregated maximum controllable VESSs power is transferred from lower level to upper level. In contrast, the dotted blue line means the control signal from upper level is transferred to lower level for selectively charging/discharging VESSs. It should be noted that the consensus algorithm convergence time depends on system size and communication networks. The updating interval in this work is much more than enough for the proposed algorithm to achieve equilibrium.
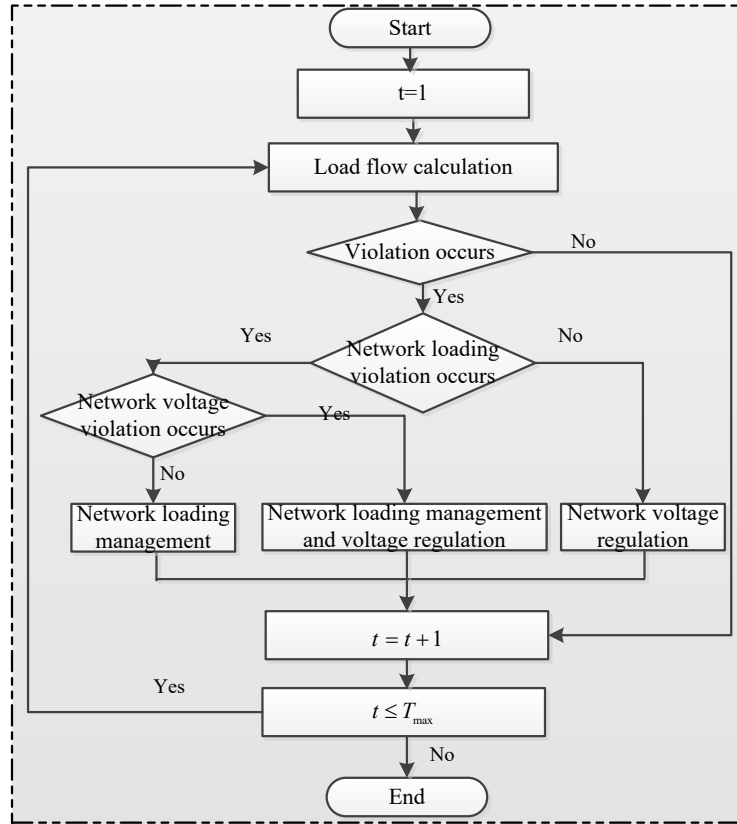
Fig. 3. Operating conditions for network loading management and voltage regulation.

11
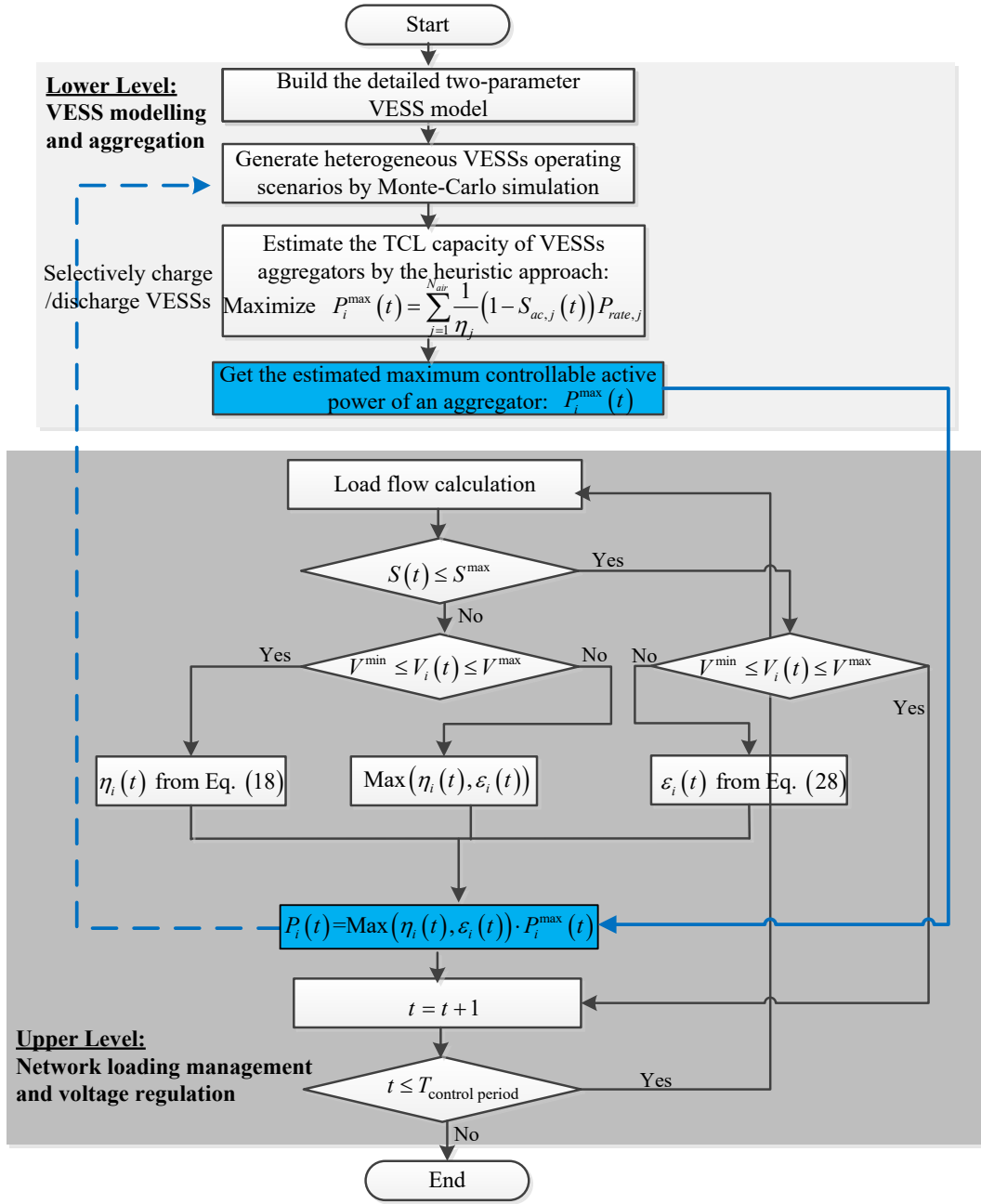
Fig. 4. Flowchart of proposed control scheme for network loading management and voltage regulation.

4. Case studies

One 11 kV nine-node feeder, which approximately supplies 1000 residential and commercial customers in New South Wales, Australia [39], is used in this case study to demonstrate the performance of proposed control scheme. It is estimated that more than 75% of households along the feeder have at least one air-conditioner installed. The one-line diagram of nine-node test feeder is shown in Fig. 5, with connected PV systems and aggregators in the network.

There is one virtual leader and five aggregators, with 150 air conditioners regulated by each aggregator, distributed across the system. The heterogeneous VESS models are generated by Monte-Carlo simulation method, with parameters sampling ranges provided in Table 1. In this work, the thermal resistance of VESS includes glass

windows and walls, which is calculated as a lump-sum resistance. The thermal capacitance of walls is considered as well.
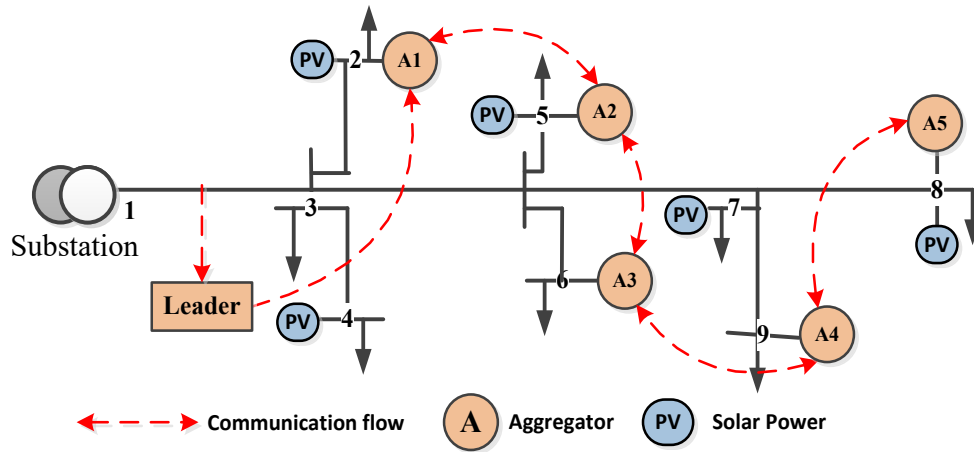
Fig. 5. One-line diagram of nine-node test feeder.

Table 1 VESS parameters sampling ranges for Monte-Carlo simulation.

House Length/m	House Width/m	House Height/m
8-22	10-20	3-9
Wall Width/m	**Set Point of Thermostat/ °C**	**No. of Windows**
0.2-0.4	23-26	3-8
Air Conditioners Rated Power/kW		
1-7		

Differential evolution (DE) algorithm is employed in this paper to solve the maximum active power estimation model in (14). The maximum iteration time and population size are both fixed as 100 in DE algorithm. The detailed DE algorithm process is omitted here, which can be found in a similar work in [40]. Different temperature deadband scopes are given for the aggregators to simulate different households thermal comfort preferences. In this work, the temperature deadband scopes for five aggregators are 1 ℃, 2 ℃, 3 ℃, 4 ℃ and 5 ℃. By solving the model in (14), the maximum controllable capacity of each VESSs aggregator in one day is denoted in Fig. 6. In actual situations, a variety of factors influences the capacity of VESSs, such as building parameters (e.g. building material characteristics and room volume), meteorological parameters (e.g. indoor temperature and ambient temperature), and human parameters (e.g. temperature deadband scopes and ideal temperature set points). As observed from Fig. 6, the larger temperature deadband scopes are, the more maximum controllable capacity each VESSs aggregator has.
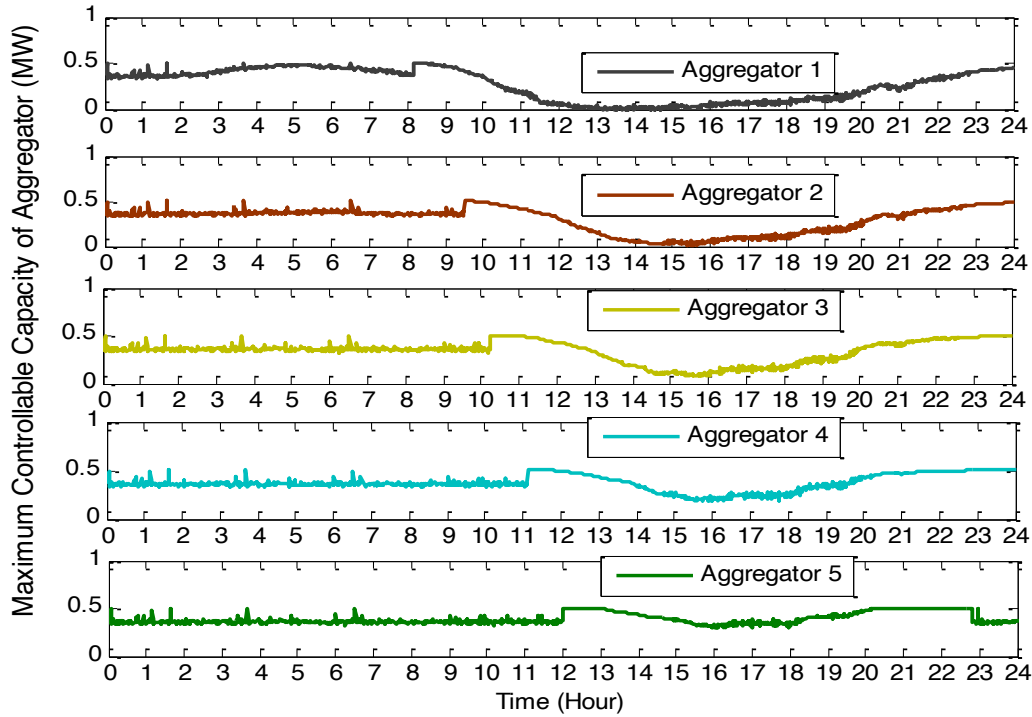
Fig. 6. VESSs aggregator maximum controllable capacity in one day.

The substation contains one transformer with summer rating being 3.3 MVA and the secondary transformer voltage at local nodes is 230 V, which is regarded as 1.0 p.u. (per unit). The maximum voltage limit is set as 1.05 p.u. and the minimum voltage limit is set as 0.96 p.u. Therefore, to guarantee the system normal operation, the system voltage should be controlled between the minimum and the maximum limits, and the network loading should be no larger than 3.3 MVA. The rated PV capacity in each node is denoted in Table 2, where one-minute solar radiance resolution data is derived based on a typical summer data in UQ Solar Photovoltaic Centre to get the daily PV power profile [41]. The system load is predicted based on the classical residential load demand in [42].

Table 2 Rated capacity in each node of the system.

Node	2	4	5	7	8
PV Capacity (MW)	0.36	0.45	0.52	0.54	0.48

4.1. Case 1

In this case study, the performance of proposed control scheme is verified. The simulation program is conducted in MATLAB on a 4 core, 64-bit DELL Desktop with Intel Core i5-3570S CPU and 8 giga-byte RAM.

Fig. 7(a) demonstrates the system node voltage change in one day under high PV power penetration and peak residential electricity demand. It can be found that the voltage in local nodes keeps rising because of PV penetration into the system, and crosses the maximal voltage limit during 8:30-14:30. Compared with overvoltage, undervoltage occurs during 19:00-21:00 because of the high residential electricity demand. Once the voltage violation happens, the proposed control scheme is initiated to regulate system voltage by the smart coordination of aggregated VESSs.

14

Observing the grey line in Fig. 8, it can be clearly seen that system apparent power crosses summer rating value from 18:30 to 21:30. This is caused by the peak electricity demand in hot summer days when residents are back to home from work, especially caused by turning on the large amount of air conditioners. Similar to voltage regulation, once overloading occurs, the proposed control strategy is implemented to manage system loading.
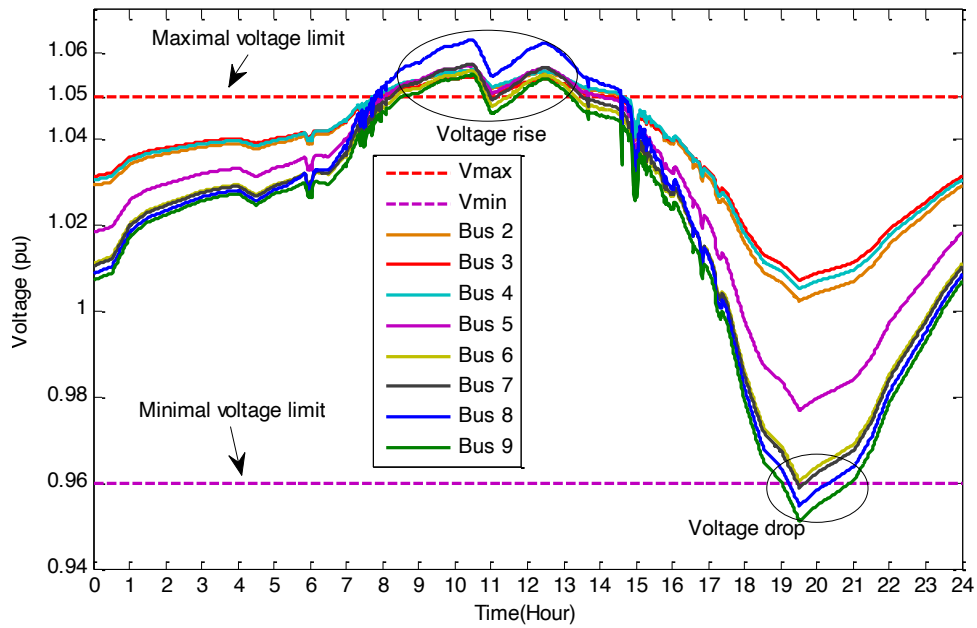
(a) voltage profile before control.
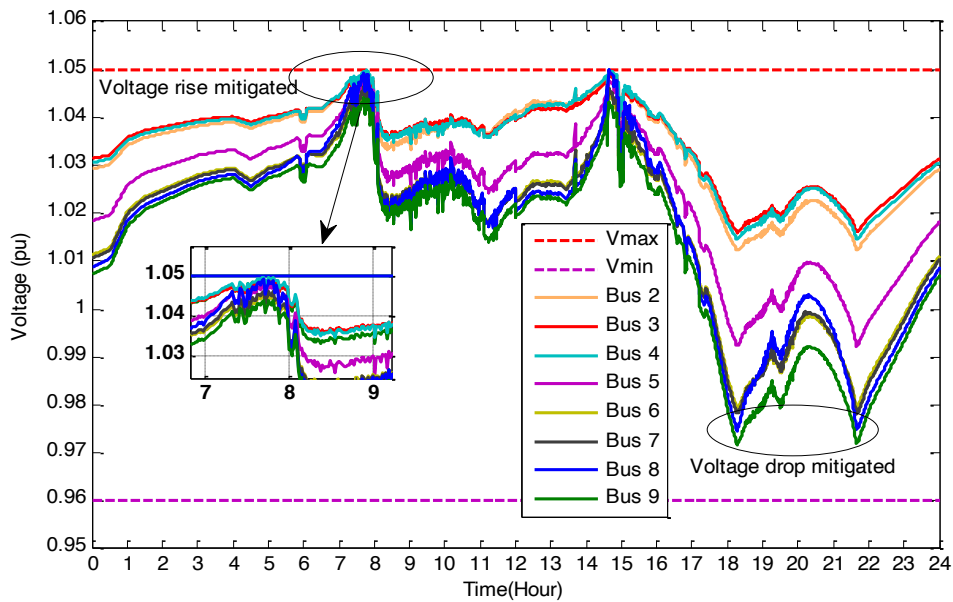
(b) voltage profile after adopting proposed control scheme.

Fig. 7. Voltage profile in one day (a) voltage profile before control. (b) voltage profile after adopting proposed control scheme.
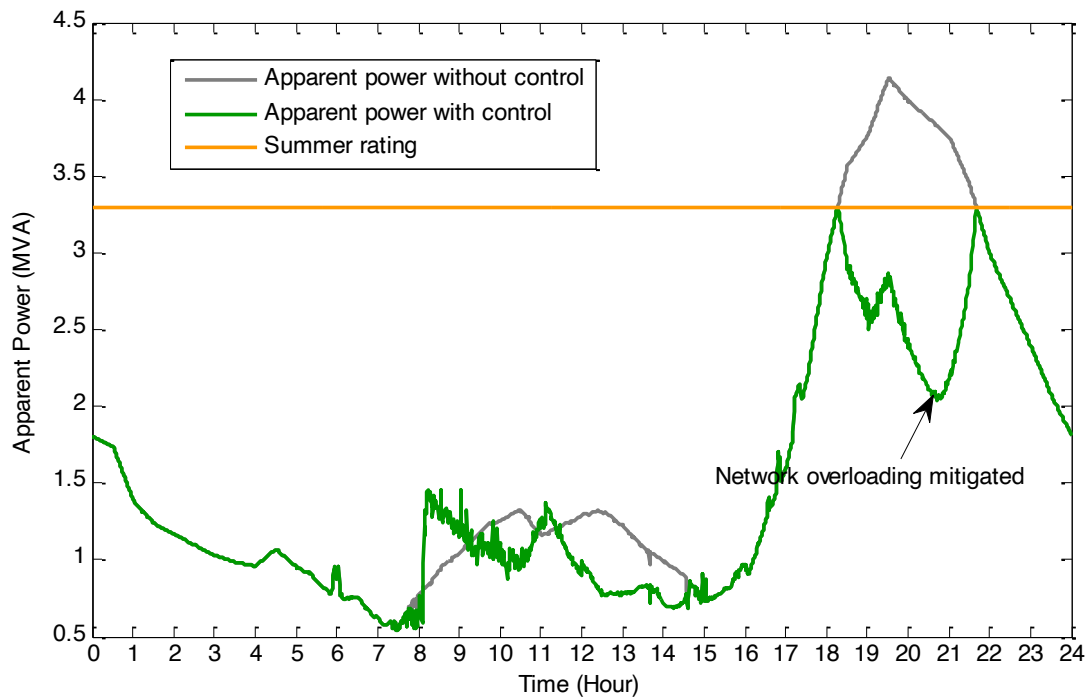
Fig. 8. Network loading change in one day without and with control.

Fig. 7(b) demonstrates the voltage control performance by the proposed strategy. With the proposed control scheme, the nodes voltage is maintained within the desirable range during the day. Specifically, from 8:30-14:30, voltage rise is mitigated and is controlled to be no more than 1.05 p.u.. This control effect is achieved by the extra consumption of PV generation by turning on VESSs, hence the reverse power from PV inverters into distribution network are reduced. From 19:00 to 21:00, voltage drop is eliminated as well and kept larger than the minimal voltage limit, i.e. 0.96 p.u.. During these periods, VESSs are turned off to help reducing electricity demand.

Fig. 8 shows the network loading control performance. It can be observed that the system overloading is well controlled below the summer rating value from 18:30 to 21:30, which is achieved by the reduced electricity consumption via selectively turning off VESSs. Given that VESSs are required to turn off during both under-dervoltage periods and overloading periods, a larger active power control value should be executed during these two periods, which can guarantee the overall system control performance.

The contribution amount of each VESSs aggregator is denoted in Fig. 9. The VESSs work in charging mode, i.e. VESSs are turned on, during high PV penetration periods to help lower nodal voltage. During 18:30-21:30, VESSs work in discharging mode, i.e. VESSs are turned off, to compensate voltage drop and network overloading. It should be noted that by considering indoor air temperature restrictions (shown in (11)), the thermal comfort in residential household is not compromised during the whole control period.

16
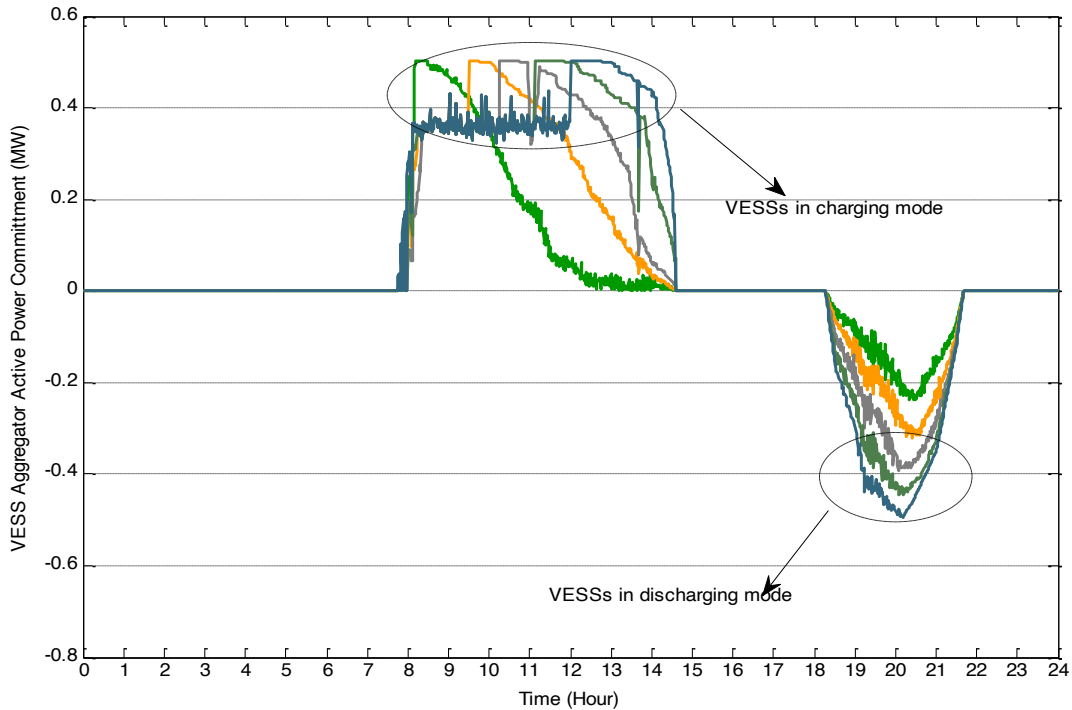
Fig. 9. VESSs aggregator active power contribution.

4.2.   Case 2

Given the communication channel disturbance in Equation (16), different communication topology networks can be formed among aggregators, which could cause impacts on the algorithm convergence. Therefore, the influence of dynamic communication topology on system performance is investigated in this part to demonstrate the robustness of proposed control scheme.

The common adopted communication topologies for the aggregators are line shape, star shape, ring shape, and complete shape. Figs. 10-12 separately present the star topology, complete topology and ring topology, together with the voltage control performances. For network loading effects under different topologies, these three topologies have similar control results to line topology shown in Fig. 8. Therefore, only the network loading management performance under ring topology is given here for reference. The control results under line shape topology have been given in Case 1. Four different communication network topologies all demonstrate satisfying system control performances, which verify the control scheme robustness in terms of dynamic network topologies. The control scheme calculation speed and system performance of these four communication network topologies are summarized in Table 3.

It is worth noting that complete network topology shows the fastest calculation speed, owing to faster consensus algorithm convergence speed compared with the other three topologies. On the other hand, complete topology has the most sophisticated communication channels, which also increase the communication cost dramatically. It can also be observed that ring topology and complete topology are robust to communication failures. When one communication link is removed among aggregators, the system control performance will not be affected. Combining calculation speed and communication costs, the ring topology is more ideal from the system operator's perspective, with relatively fast computation speed and less communication line investment.
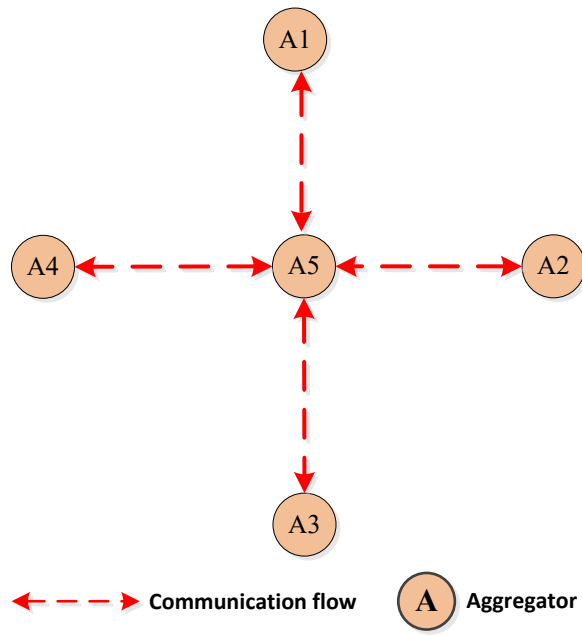
(a)　Star shape topology.
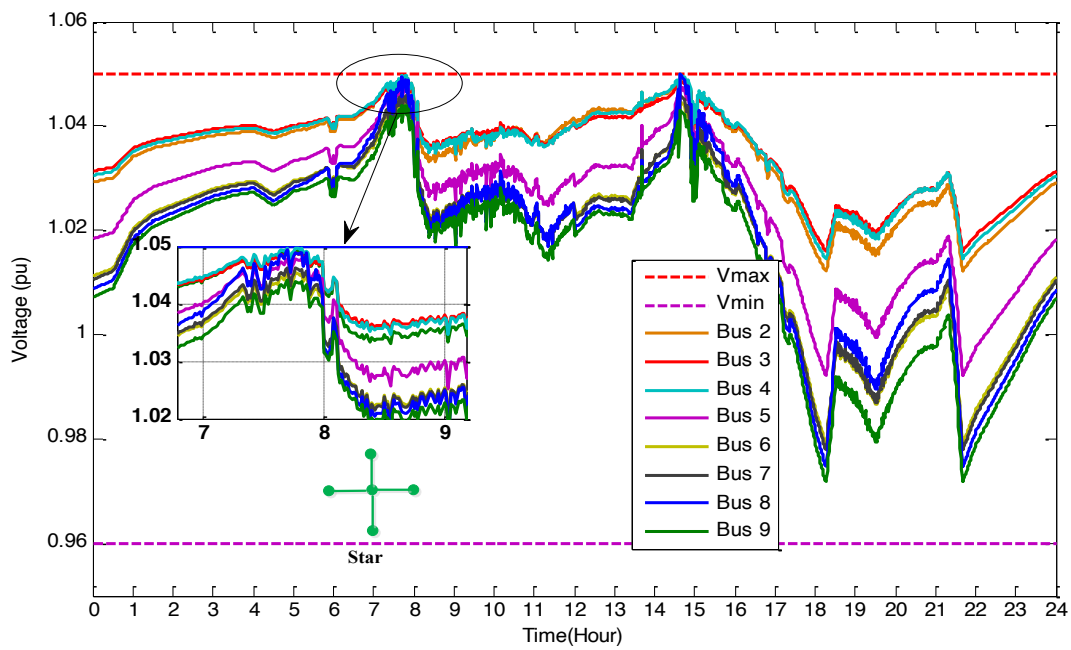
(b)　Voltage performance under Star shape topology.

Fig. 10 Voltage performance under Star shape topology (a) Star shape topology. (b) Voltage regulation performance under Star shape topology.
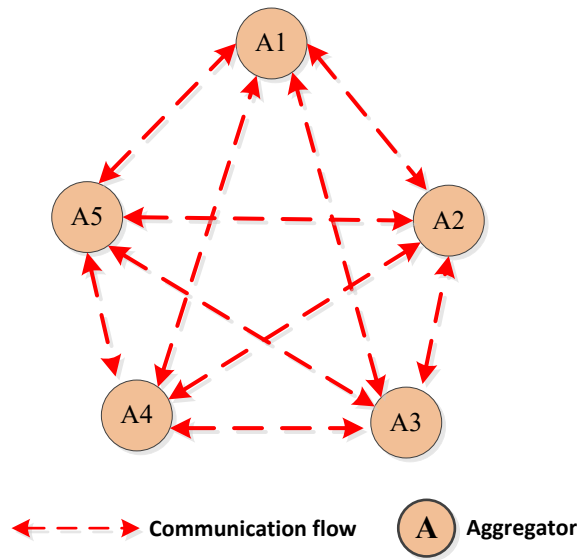
(a) Complete shape topology.
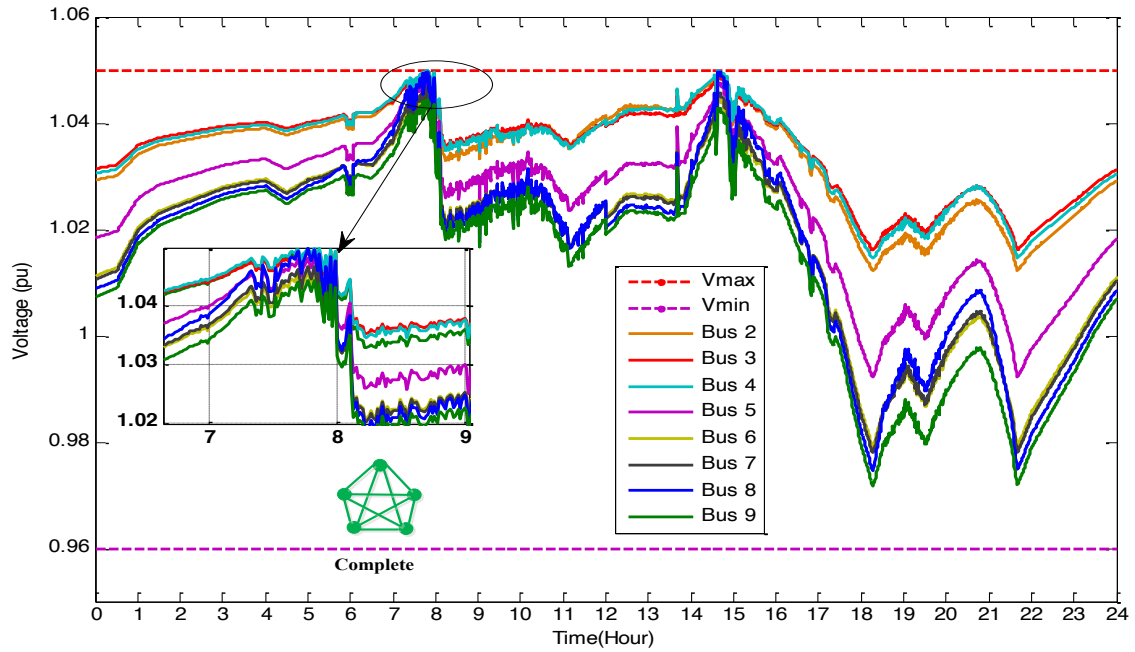
(b) Voltage performance under Complete shape topology.

Fig. 11. Voltage regulation performance under Complete shape topology (a) Complete shape topology (b) Voltage regulation performance under Complete shape topology.
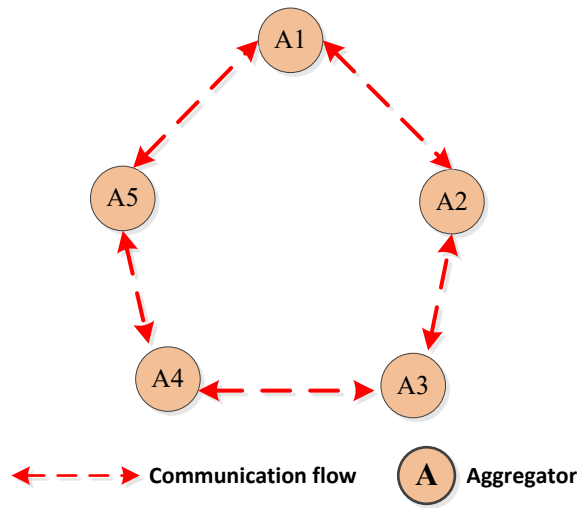
(a) Ring shape topology.
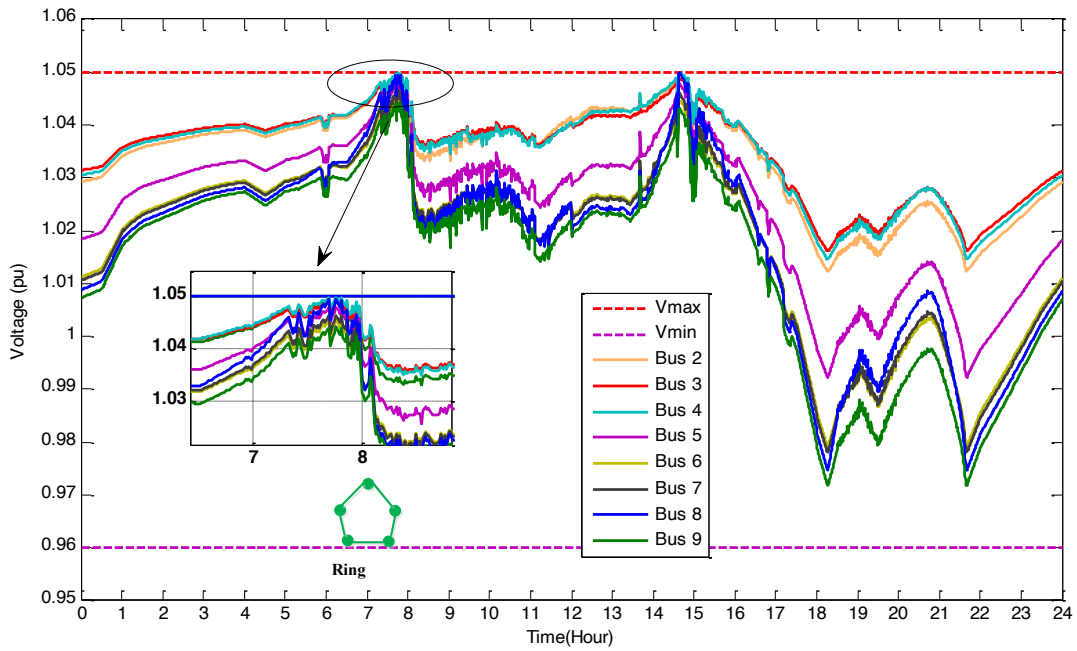
(b) Voltage performance under Ring shape topology.
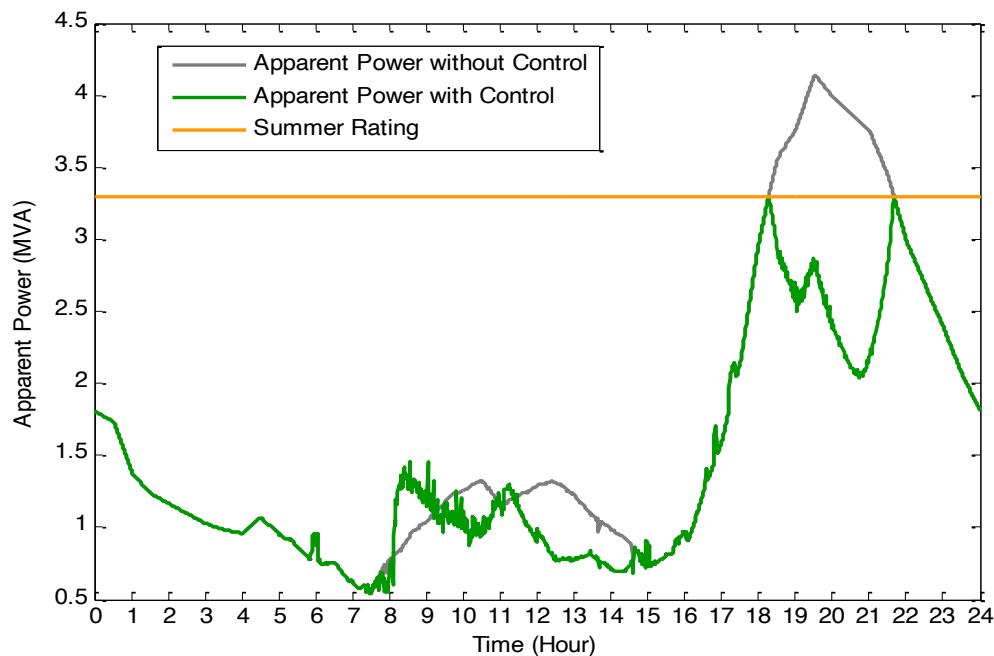
(c)   Network loading management under Ring shape topology.

Fig. 12. Voltage regulation performance and network loading management performance under Ring shape topology (a) Ring shape topology (b) Voltage regulation performance under Ring shape topology (c) Network loading management performance under Ring shape topology.

Table 3 Calculation speed and system performance for different network topologies.

Network topology	Calculation speed (seconds)	Voltage regulation effectiveness	Network loading management effectiveness	Robust to communication failure
Line	29.02	Yes	Yes	No
Star	23.24	Yes	Yes	No
Ring	17.95	Yes	Yes	Yes
Complete	15.74	Yes	Yes	Yes

5. Conclusions and Future Work

A smart coordination strategy is proposed in this paper to coordinate aggregated VESSs for distribution network voltage regulation and loading management. Through the lower level control, the VESS model is built and the aggregated amount of maximum controllable active power is calculated. Through the upper level control strategy, a consensus-driven distributed control strategy is employed to fairly share the active power commitment among aggregators for distribution network management. The simulation results on a nine-node test feeder in New South Wales prove the effectiveness of proposed control scheme, as well as demonstrate the robustness in case of dynamic communication network topologies and communication failure. The proposed method is superior over other methods in terms of, 1) utilizing the thermal buffering capacity of air-conditioned households to form VESSs, with far less cost than hard energy storage techniques; 2) reaping demand response programs benefits via aggregators, with end-users' thermal comfort guaranteed; 3) adapting to dynamic communication network topologies, in the meanwhile ensuring the equilibrium point is reached among participating aggregators. With the increasing penetration of renewable resources and deployment of smart household energy management systems,

the proposed method is believed to be a promising method on managing practical distribution networks in a techno-economic manner.

Future work will focus on improving the thermal modelling of virtual energy storage system by considering other important factors, including solar irradiance and window area. In addition, the VESSs control in large-scale systems with complex communication network will be investigated.

Acknowledgements

References

[1]   International Energy Agency, "Renewables 2018", [Online] Available: https://www.iea.org/renewables2018/(Accessed13/10/2019)

[2]   H. Akagi and K. Isozaki, "A hybrid active filter for a three-phase 12-pulse diode rectifier used as the front end of a medium-voltage motor drive," *IEEE Trans. Power Electron.*, vol. 27, no. 4, pp. 1758-1772, Apr. 2012.

[3]   M. Zeraati, M. E.H. Golshan, and J. M. Guerrero, "Distributed control of battery energy storage systems for voltage regulation in distribution networks with high PV penetration," *IEEE Trans. Smart Grid*, vol. 9, no. 4, pp. 3582-3593, July 2018.

[4]   F. H. M. Rafi, M. J. Hossain, and J. Lu, "Hierarchical controls selection based on PV penetrations for voltage rise mitigation in a LV distribution network," *International Journal of Electrical Power & Energy Systems*, vol. 81, pp. 123–139, Oct. 2016.

[5]   M. R. Salem, L. A. Talat, and H. M. Soliman, "Voltage control by tap changing transformers for a radial distribution network," *Proc. Inst. Elect. Eng., Generation Transmission and Distribution,* 1997, vol. 144, pp. 517-520.

[6]   C. L. Masters, "Voltage rise: The big issue when connecting embedded generation to long 11kV overhead lines," *Power Engineering Journal*, vol. 16, pp. 5-12, 2002.

[7]   M. Tonkoski, "Transformer voltage regulation-compact expression dependent on tap position and primary /secondary voltage," *IEEE Trans. Power Delivery*, vol. 29, no. 3, pp. 1516–1517, Apr. 2014.

[8]   C. S. Chen, C. Lin, W. Hsieh, C. T. Hsu, T. T. Ku, "Enhancement of PV penetration with DSTATCOM in Taipower distribution system," *IEEE Trans. Power Syst.*, vol. 28, no. 2, pp. 1560–1567, May 2013.

[9]   R. Tonkoski and L. A. C. Lopes, "Impact of active power curtailment on overvoltage prevention and energy production of PV inverters connected to low voltage residential feeders," *Renewable Energy*, vol. 36, no. 12, pp. 3566–3574, Dec. 2011.

[10]   S. Ghosh, S. Rahman, and M. Pipattanasomporn, "Distribution voltage regulation through active power curtailment with PV inverters and solar generation forecasts," *IEEE Trans Sustainable Energy*, vol. 8, no. 1, pp. 13-22, Jan. 2017.

[11]   Y. Wang, K. Tan, X. Peng, and P. So, "Coordinated control of distributed energy-storage systems for voltage regulation in distribution networks," *IEEE Trans. Power Delivery*, vol. 31, no.3, pp. 1132-1141, June 2016.

[12]   X. Yan, C. Gu, F. Li, and Y. Xiang, "Network pricing for customer-operated energy storage in distribution networks," *Applied Energy*, vol. 212, pp. 283–292, Feb. 2018.

[13]   A. S. Sidhu, M. G. Pollitt, and K. L. Anaya, "A social cost benefit analysis of grid-scale electrical energy storage projects: a case study," *Applied Energy,* vol. 212, pp. 861–894, Feb. 2018.

[14]   C. S. Lai and M. D. McCulloch, "Levelized cost of electricity for solar photovoltaic and electrical energy storage," *Applied Energy,* vol. 190, pp. 191–203, March 2017.

[15]   D. Wang, K. Meng, F. Luo, C. Coates, X. Gao, Z. Y. Dong, "Coordinated dispatch of networked energy storage systems for loading management in active distribution networks", *IET Renewable Power Generation*, vol. 10, no. 9, pp. 1374-1381, Oct. 2016.

[16] R. Smith, K. Meng, Z. Y. Dong, and R. Simpson, "Demand response: A strategy to address residential air-conditioning peak load in Australia," *J. Mod. Power Syst. Clean Energy*, vol. 1, no. 3, pp. 223-230, Nov. 2013.

[17] F.A. Rahiman, H.H. Zeineldin, V. Khadkikar, S.W. Kennedy, and V.R. Pandi, "Demand response mismatch (DRM): concept, impact analysis, and solution," *IEEE Trans. Smart Grid*, vol. 5, no. 4, pp. 1734–1743, Jul. 2014.

[18] F. Y. Xu, T. Zhang, L. L. Lai and H. Zhou, "Shifting boundary for price-based residential demand response and applications," Applied Energy, Elsevier, 146, pp. 353–370, 2015.

[19] C. S. Lai, F. Xu, M. McCulloch and L. L. Lai, "Application of distributed intelligence to industrial demand response," Chen-Ching Liu, Stephen McArthur and Seung-Jae Lee (Editors), *Smart Grid Handbook*, IEEE Press & Wiley, 2016.

[20] A. Ihsan, M. Jeppesen, M. J. Brear, "Impact of demand response on the optimal, techno-economic performance of a hybrid, renewable energy power plant", *Applied Energy*, vol. 238, pp. 972-984, March 2019.

[21] D. Wang, K. Meng, X. Gao, C. Coates, and Z. Y. Dong, "Optimal air-conditioning load control in distribution network with intermittent renewables", *J. Mod. Power Syst. Clean Energy,* vol. 5, no. 1, pp. 55-65, Jan. 2017.

[22] M. Cheng, S. S. Sami, and J. Wu, "Benefits of using virtual energy storage system for power system frequency response," *Applied Energy*, vol. 194, pp. 376–385, May 2017.

[23] A. Busic, "Virtual energy storage through distributed control of flexible loads," *California France Forum on Energy Efficiency Technologies*, San Francisco, CA, Sep. 2015.

[24] S. Akagi, S. Yoshizawa, etc. "Multipurpose control and planning method for battery energy storage systems in distribution network with photovoltaic plant", *International Journal of Electrical Power & Energy Systems,* vol. 116, March 2020

[25] I. Ranaweera, O. M. Midtgard, and M. Korpas, "Distributed control scheme for residential battery energy storage units coupled with PV systems," *Renewable Energy*, vol. 113, pp. 1099-1110, Dec. 2017.

[26] L. Wang and B. Chen, "Distributed control for large-scale plug-in electric vehicle charging with a consensus algorithm" *International Journal of Electrical Power & Energy Systems,* vol. 109, pp. 369-383, July 2019.

[27] W. Liu, W. Gu, Y. Xu, S. Xue, and M. Fan, "Improved average consensus algorithm based distributed cost optimization for loading shedding of autonomous microgrids," *International Journal of Electrical Power & Energy Systems*, vol. 73, pp. 89-96, Dec. 2015

[28] X. Wu, C. Shen, and R. Iravani, "A distributed cooperative frequency and voltage control for microgrids," *IEEE Trans. Smart Grid*, vol. 9, no. 4, pp.2764-2776, July 2018.

[29] H. Xin, Y. Liu, Z. Qu, and D. Gan, "Distributed control and generation estimation method for integrating high-density Photovoltaic systems," *IEEE Trans. Energy Convers.*, vol. 29, no. 4, pp. 988–996, Dec. 2014

[30] S. Bashash and H.K. Fathy, "Modeling and control of aggregate air conditioning loads for robust renewable power management," *IEEE Trans. Cont. Syst. Tech.*, vol. 21, no. 4, pp. 1318–1327, Jul. 2013.

[31] N. Lu and Y. Zhang, "Design considerations of a centralized load controller using thermostatically controlled appliances for continuous regulation reserves," *IEEE Trans. Smart Grid*, vol. 4, no. 2, pp. 914–921, Jun. 2013.

[32] H. Wang, K. Meng, Z. Dong, F. Luo, Z. Xu, G. Verbic, and K. P. Wong, "Demand response through smart home energy management using thermal inertia," *Australian Universities Power Engineering Conference,* Hobart, Australia, 2013.

[33] A. Talwariya, P. Singh, M. Kolhe, "A stepwise power tariff model with game theory based on Monte-Carlo simulation and its applications for household, agricultural, commercial and industrial consumers", *International Journal of Electrical Power & Energy Systems,* vol. 111, pp. 14-24, Oct. 2019

[34] C.-S. Karavas, G. Kyriakarakos, K.G. Arvanitis, G. Papadakis, "A multi-agent decentralized energy management system based on distributed intelligence for the design and control of autonomous polygeneration microgrids," *Energy Conversion and Management*, vol. 103, pp.166–179, October 2015.

[35] R. O. Saber and R. M. Murray, "Consensus problems in networks of agents with switching topology and time-delays," *IEEE Transactions on Automatic Control*, vol. 49, no. 9, pp. 1520-1533, Sep. 2004.

[36] W. He, G. Chen, Q. Han, and F. Qian, "Network-based leader-following consensus of nonlinear multi-agent systems via distributed impulsive control," *Information Sciences*, vol. 380, pp. 145-158, Feb. 2017.

[37] R. Olfati-Saber, J. Fax, and R.M. Murray, "Consensus and cooperation in networked multi-agent systems," *Proc. IEEE*, vol. 95, no. 1, pp. 215–233, Jan. 2007.

[38]   K. K. Mehmood, S. U. Shan, et.al, "A real-time optimal coordination scheme for the voltage regulation of a distribution network including an OLTC, capacitor banks, and multiple distributed energy resources," *International Journal of Electrical Power & Energy Systems*, vol. 94, pp. 1-14, Jan. 2018.

[39]   K. Meng, Z. Y. Dong, Z. Xu, Y. Zheng, and D. J. Hill, "Coordinated dispatch of virtual energy storage systems in smart distribution networks for loading management," *IEEE Trans. Systems, Man, and Cybernetics: Systems*, April 2017, in press.

[40]   F. Luo, Z.Y. Dong, K. Meng, J. Wen, H. Wang, and J. Zhao, "An operational planning framework for large scale thermostatically controlled load dispatch," *IEEE Trans. Ind. Informat.*, vol. 13, no. 1, pp. 217-227, Feb. 2017.

[41]   UQ   SOLAR   Photovoltaic   Data,   [Online].   Available: http://solar.uq.edu.au/user/reportPower.php?dtra=day&dts=2015-11-26 (accessed 03/10/2019).

[42]   A. J. Jardini, C. M. V. Tahan, M. R. Gouvea, S. U. Ahn, and F. M. Figueiredo, "Daily load profiles for residential, commercial, and industrial low voltage consumers," *IEEE Trans. Power Delivery*, vol. 15, no. 1, pp. 375–380, Jan. 2000.